Theoretical Study of the Reactivity of (π-Allyl)molybdenum Complexes

Tomohiro Suzuki, Goro Okada, Yasunori Hioki, and Hiroshi Fujimoto*

Division of Molecular Engineering, Kyoto University, Kyoto 606-8501, Japan

Received September 9, 2002

The reactivity of allyl carbons in (π-allyl)molybdenum complexes has been investigated theoretically. The central carbon of the allyl moiety has been shown to be more reactive than the terminal carbons toward nucleophiles in $Cp_2Mo(\eta^3\text{-allyl})^+$ by locating a reactant complex, transition states, and products with the density functional theoretical calculations. Orbital interactions have been analyzed then by applying a paired interacting orbital scheme to the MO wave function. The local electron-accepting ability of allyl carbons has been evaluated, showing that the acidic hardness of reaction sites is a key to understand the higher reactivity of the central carbon. The regioselectivity observed in nucleophilic attacks to $CpMo(\eta^3\text{-allyl})(CO)(NO)^+$ and some other (π-allyl)molybdenum complexes has also been investigated in terms of the local electron-accepting ability of the reaction sites. The terminal carbons are shown to be more reactive in these cases.

Introduction

A number of useful synthetic methods using allyl complexes of transition metals have been developed to attain highly selective reactions. For example, palladium-catalyzed allylic alkylation has been utilized as a method of enantioselective synthesis.[1,2] π-Allyl palladium complexes give several types of π-allyl templates, taking in most cases the square-planer 16-electron structures.[2,3] On the other hand, π-allyl complexes of the group VI metals give a variety of π-allyl templates which can be utilized effectively for synthetic purposes.[2,4] Particularly, (π-allyl)molybdenum and (π-allyl)-tungsten complexes have attracted much attention, because of their wide availability and also of their extraordinarily high chemo-, regio-, and stereoselectivities.[5−9] Nucleophilic addition to organotransition metal cations containing unsaturated hydrocarbon ligands is systematically rationalized by the Davis−Green−Mingos (DGM) rules, which have remarkable and successful applications.[2a,10]

In the reactions of a cationic (π-allyl)molybdenum complex, $CpMo(\eta^3\text{-allyl})(CO)(NO)^+$, nucleophiles attack preferentially the terminal carbons of allyl moiety to give olefins.[5a,c−h,6] Faller et al. found a remarkable stereoselectivity in nucleophilic additions.[5] Equilibrium between two conformational isomers, *endo* and *exo*, has been suggested.[5,6,11] The product olefin complexes of these reactions have been detected in two diastereoisomeric forms which take the absolute configurations of olefins shown in Scheme 1.[5a] The regioselectivity observed in the reaction of $CpMo(\eta^3\text{-allyl})(CO)(NO)^+$ was explained by Hoffmann in terms of the MO coefficients and charges of allyl carbons, based on the fragment molecular orbital (FMO) analysis.[12] It was also pointed out that the central carbon of these complexes was less reactive, because of a weaker overlap between the allyl carbon and an attacking nucleophile.

In contrast, in dicyclopentadienyl complex $Cp_2Mo(\eta^3\text{-allyl})^+$, nucleophiles are known to attack preferentially the central carbon of an allyl unit to give metallacyclobutanes, as illustrated in Scheme 2.[9,13] Eisenstein et al. showed that the symmetric MO 3a′ in the extended Hückel MO theory, which might feature the acceptor

(1) (a) Tsuji, J. *Organic Synthesis with Palladium Compounds*; Springer-Verlag: New York, 1980. (b) Trost, B. M.; Verhoeven, I. R. In *Comprehensive Organometallic Chemisty*; Wilkinson, G., Ed.; Pergamon Press: Oxford, 1982; Vol. 8, p 1779. (c) Consiglio, G.; Waymouth, R. M. *Chem. Rev.* **1989**, *89*, 257. (d) Trost, B. M.; Van Vranken, D. L. *Chem. Rev.* **1996**, *96*, 395.

(2) (a) Collman, J. P.; Hegedus, L. S.; Norton, J. R.; Finke, R. G. *Principles and Applications of Organotransition Metal Chemistry*; University Science Books: Mill Valley, CA 1987. (b) L. C. L.; Liu, R. S. *Chem. Rev.* **2000**, *100*, 3127.

(3) Huheey, J. E.; Keiter, E. A.; Keiter, R. L. *Inorganic Chemistry: Principles of Structure and Reactivity*; Harper Collins College Publishers: New York, 1993.

(4) Davis, R.; Kane-Maguire, L. A. P. In *Comprehensive Organometallic Chemistry*; Wilkinson, G., Ed.; Pergamon Press: Oxford, 1982; Vol. 3, p 1149, 1321.

(5) (a) Faller, J. W.; Rosan, A. M. *J. Am. Chem. Soc.* **1976**, *98*, 3388. (b) Faller, J. W.; Rosan, A. M. *J. Am. Chem. Soc.* **1977**, *99*, 4858. (c) Adams, R. D.; Chodosh, D. F.; Faller, J. W.; Rosan, A. M. *J. Am. Chem. Soc.* **1979**, *101*, 2570. (d) Faller, J. W.; Chao, K. H. *J. Am. Chem. Soc.* **1983**, *105*, 3893. (e) Faller, J. W.; Chao, K. H. *Organometallics* **1984**, *3*, 927. (f) Faller, J. W.; Chao, K. H.; Murray, H. H. *Organometallics* **1984**, *3*, 1231. (g) Faller, J. W.; Lambert, C. *Tetrahedron* **1985**, *41*, 5755. (h) Faller, J. W.; Lambert, C.; Mazzieri, M. R. *J. Organomet. Chem.* **1990**, *383*, 161.

(6) (a) VanArsdale, W. E.; Winter, R. E. K.; Kochi, J. K. *J. Organomet. Chem.* **1985**, *296*, 31. (b) VanArsdale, W. E.; Winter, R. E. K.; Kochi, J. K. *Organometallics* **1986**, *5*, 645. (c) VanArsdale, W. E.; Kochi, J. K. *J. Organomet. Chem.* **1986**, *317*, 215.

(7) (a) Trost, B. M.; Lautens, M. *J. Am. Chem. Soc.* **1982**, *104*, 5543. (b) Trost, B. M.; Lautens, M. *J. Am. Chem. Soc.* **1983**, *105*, 3343. (c) Trost, B. M.; Lautens, M. *Organometallics* **1983**, *2*, 1687.

(8) Trost, B. M.; Hung, M. H. *J. Am. Chem. Soc.* **1983**, *105*, 7757.

(9) (a) Ephritikhine, M.; Green, M. L. H.; MacKenzie, R. E. *J. Chem. Soc., Chem. Commun.* **1976**, 619. (b) Ephritikhine, M.; Francis, B. R.; Green, M. L. H. Mackenzie, R. E.; Smith, M. J. *J. Chem. Soc., Dalton Trans.* **1977**, 1131.

(10) Davis, S. G.; Green, M. L. H.; Mingos, D. M. P. *Tetrahedron* **1978**, *34*, 3047.

(11) (a) Faller, J. W.; Shvo, Y.; Chao, K.; Murray, H. H. *J. Organomet. Chem.* **1982**, *226*, 251. (b) Cosford, N. D. P.; Liebeskind, L. S. *Organometallics* **1994**, *13*, 1498.

(12) Schilling, B. E. R.; Hoffmann, R.; Faller, J. W. *J. Am. Chem. Soc.* **1979**, *101*, 592.

10.1021/om0207459 CCC: $25.00
Publication on Web 08/05/2003

Scheme 1

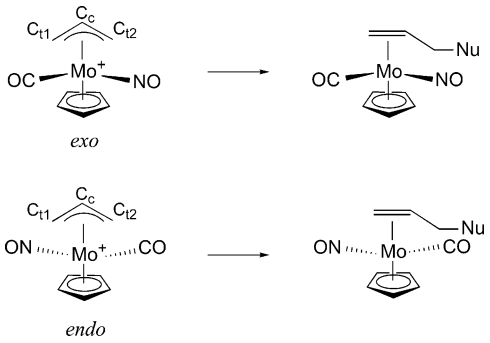

Scheme 2

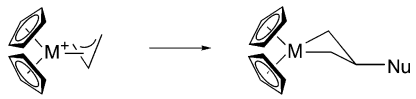

M = Mo, W

site on the central carbon, C_c, was located slightly below the antisymmetric MO 2a″, which would direct the nucleophile to the terminal carbons, C_{t1} and C_{t2}, in $Cp_2M(\eta^3\text{-allyl})^+$.[14,15] They pointed out that the central carbon was charged more positive relative to the terminal carbons, so that the charge and frontier orbital controls would work in concert to direct the nucleophile to the central carbon in this system. It is supposed, however, that both the 3a′ and 2a″ MOs of an allyl moiety participate significantly in interaction between a terminal carbon and a nucleophile, when a nucleophile attacks one of the terminal carbons of (π-allyl)molybdenum complexes.

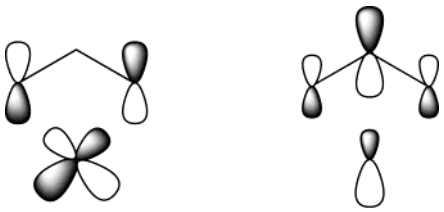

The regioselectivity in the nucleophilic additions to η^3-allyl molybdenum complexes has been studied theoretically.[12,14,16] It was suggested that the MO coefficients of allyl carbons would govern the regioselectivity of nucleophilic additions to $CpMo(\eta^3\text{-allyl})(CO)(NO)^+$ and $Mo(\eta^3\text{-allyl})(CO)_2(PH_3)_n^+$ (n = 2, 3).[12,14] On the other hand, the symmetry of the frontier orbital was pointed out to be of importance in the reaction of $Cp_2M(\eta^3\text{-allyl})^+$ complexes.[14] Trost et al. examined the electronic charges and the amplitude of the LUMO on the carbons in model cationic species derived from polyene substrates to discuss the regioselectivity in nucleophilic additions to π-allyl metal complexes.[16]

We have studied the reactivity of the allyl carbons of η^3-allyl platinum and palladium complexes.[17] Using a concept of paired interaction orbitals and the local electron-accepting ability of the reaction sites, we successfully clarified that the reactivities of allyl carbons are mainly controlled by d orbital in the 2a″ MO. From this result, one can expect that the concept of paired interaction orbitals and the local electron-accepting ability of the reaction site are very powerful to investigate the reactivity of η^3-allyl molybdenum complexes mentioned above. In this work, we theoretically investigated the reactivity of (π-allyl)molybdenum complexes, by means of density functional theoretical calculations and by applying the concept of paired interaction orbitals and local electrophilicity of the reaction sites.[18−20] Our intention in this study is to provide a unifying scale to understand and predict the reactivity of the metal complexes.

Method of Calculations

Geometry optimizations were performed by applying the density functional theoretical method of Becke's three-parameters with Lee, Yang, and Parr's gradient-corrected correlation functionals (B3LYP), using the Gaussian 98 program.[21,22] Hay and Wadt's ECP2 double-ζ basis with effective core potentials (ECPs) was employed for Mo,[23] and the 3-21G basis was used for the H, C, N, and O atoms in the ligands (BS1) in $Cp_2Mo(\eta^3\text{-allyl})^+$.[24] The 6-31G basis set was used for the H, C, N, and O atoms in the calculations of $CpMo(\eta^3\text{-allyl})(CO)(NO)^+$ and other complexes. The calculated transition states were verified by vibrational frequency calculations at this level.[25] The relative energies of three $CpMo(\eta^3\text{-allyl})(CO)(NO)^+$ isomers were evaluated by B3LYP single-point calculations with another basis set in which one f-function[26] was added to the Mo primitive functions and the 6-31G* basis (BS2) and 6-311G** basis were used for H, C, N, and O atoms

(13) (a) Francis, B. R.; Green, M. L. H.; Luong-thi, T.; Moser, G. A. *J. Chem. Soc., Dalton Trans.* **1976**, 1339. (b) Green, M. L. H.; Luong-thi, T.; Moser, G. A.; Packer, I.; Pettit, F.; Roe, D. M. *J. Chem. Soc., Dalton Trans.* **1976**, 1988. (c) Green, M. L. H.; MacKenzie, R. E.; Poland, J. S. *J. Chem. Soc., Dalton Trans.* **1976**, 1993.

(14) Curtis, M. D.; Eisenstein, O. *Organometallics* **1984**, *3*, 887.

(15) Lauher, J. W.; Hoffmann, R. *J. Am. Chem. Soc.* **1976**, *98*, 1729.

(16) Trost, B. M.; Hung, M. H. *J. Am. Chem. Soc.* **1984**, *106*, 6837.

(17) Fujimoto, H.; Suzuki, T. *Int. J. Quantum Chem.* **1999**, *74*, 735.

(18) (a) Fukui, K.; Koga, N.; Fujimoto, H. *J. Am. Chem. Soc.* **1981**, *103*, 196. (b) Fujimoto, H.; Koga, N.; Hataue, I. *J. Phys. Chem.* **1984**, *88*, 3539. (c) Fujimoto, H.; Yamasaki, T.; Mizutani, H.; Koga, N. *J. Am. Chem. Soc.* **1985**, *107*, 6157. (d) Fujimoto, H.; Yamasaki, T. *J. Am. Chem. Soc.* **1986**, *108*, 578. (e) Fujimoto, H. *Acc. Chem. Res.* **1987**, *20*, 448.

(19) (a) Fujimoto, H.; Mizutani, Y.; Iwase, K. *J. Phys. Chem.* **1986**, *90*, 2768. (b) Fujimoto, H.; Satoh, S. *J. Phys. Chem.* **1994**, *98*, 1436.

(20) These orbital analyses are performed using HF wave functions, because the expansion and the orbital energy of HF wave functions are more suitable for these orbital analyses in our study. In addition, the frontier orbitals of HF wave functions, which play an important role in orbital analyses, resemble those of KS-DFT wave functions. The contour maps of HF wave functions and KS-DFT wave functions of the HOMO (80) of S3 (transition state) are drawn in the Supporting Information.

(21) Frisch, M. J.; Trucks, G. W.; Schlegel, H. B.; Gill, P. M. W.; Johnson, B. G.; Robb, M. A.; Cheeseman, J. R.; Keith, T.; Petersson, G. A.; Montgomery, J. A.; Raghavachari, K.; Al-Laham, M. A.; Zakrzewski, V. G.; Ortiz, J. V.; Foresman, J. B.; Cioslowski, J.; Stefanov, B. B.; Nanayakkara, A.; Challacombe, M.; Peng, C. Y.; Ayala, P. Y.; Chen, W.; Wong, M. W.; Andres, J. L.; Replogle, E. S.; Gomperts, R.; Martin, R. L.; Fox, D. J.; Binkley, J. S.; Defrees, D. J.; Baker, J.; Stewart, J. P.; Head-Gordon, M.; Gonzalez, C.; Pople, J. A. *Gaussian 98*; Gaussian, Inc.: Pittsburgh, PA, 1998.

(22) (a) Becke, A. D. *J. Chem. Phys.* **1993**, *98*, 5648. (b) Miehlich, B.; Savin, A.; Stoll, H.; Preuss, H. *Chem. Phys. Lett.* **1989**, *157*, 200. (c) Lee, C.; Yang, W.; Parr, R. G. *Phys Rev, B* **1988**, *37*, 785.

(23) Hay, P. J.; Wadt, W. R. *J. Chem. Phys.* **1985**, *82*, 299.

(24) Binkley, J. S.; Pople, J. A.; Hehre, W. J. *J. Am. Chem. Soc.* **1980**, *102*, 939. (b) Gordon, M. S.; Binkley, J. S.; Pople, J. A.; Pietro, W. J.; Hehre, W. J. *J. Am. Chem. Soc.* **1982**, *104*, 2797.

(25) The imaginary frequency mode is considerably localized on the reaction center, and it involves the approach of the C atom of the nucleophile to the C atom of the η^3-allyl group.

(26) Ehlers, A. W.; Böhme, M.; Dapprich, S.; Gobbi, A.; Höllwarth, A.; Jonas, V.; Köhler, K. F.; Stegmann, R.; Veldkamp, A.; Frenking, G. *Chem. Phys. Lett.* **1993**, *208*, 111.

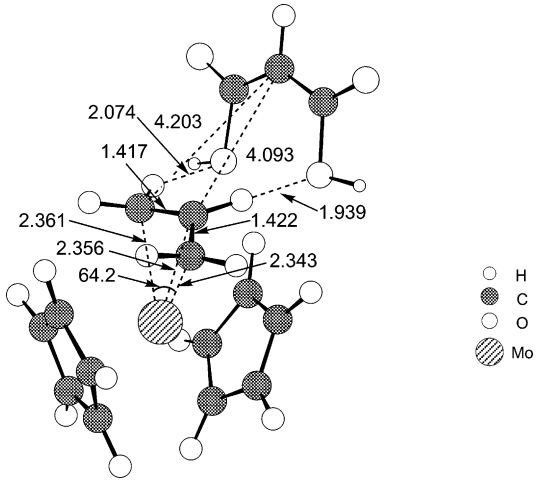

Figure 1. Stable structure of the complex between $Cp_2Mo(\eta^3\text{-allyl})^+$ and $^-CH(COOH)_2$. The bond distances are given in angstroms and the bond angles are in degrees. The energy of this structure is −983.87502 hartree, the energy of $Cp_2Mo(\eta^3\text{-allyl})^+$ is −568.98044 hartree, and the energy of $^-CH(COOH)_2$ is −414.7426 hartree in an isolated state for the B3LYP/BS1 calculations.

in the ligands (BS3),[27] with respect to the structures optimized at the B3LYP/BS1 level. Orbital analysis has been made at the RHF/BS1 level.[28]

Results and Discussion

Structures and Activation Energies. Nucleophiles may attack one of the terminal carbons to give an alkene or may attack the central carbon to give a metallacyclobutane in η^3-allyl complexes. Some differences in reactivity have been shown to exist experimentally between $CpMo(\eta^3\text{-allyl})(CO)(NO)^+$ and $Cp_2Mo(\eta^3\text{-allyl})^+$ complexes.[5c−h,6,9,13] The reactivity of carbons in allyl complexes has been discussed in terms of the unoccupied 2a″ and 3a′ MOs of the metal complex that contain respectively the π_3 and π_2 MOs of the allyl fragment as the major component.[14] The pπ AO of the central carbon has its amplitude only in the π_3 MO of an allyl, and the reactivity of the complex may be controlled by the unoccupied 3a′ MO when a nucleophile attacks the central carbon of $Cp_2Mo(\eta^3\text{-allyl})^+$. On the other hand, the pπ AO of a terminal carbon shows its amplitude both in the π_2 MO and in the π_3 MO of an allyl. The separation between the 2a″ and 3a′ MOs is not large in metal complexes, and therefore, both the 2a″ and 3a′ MOs will participate in electron delocalization when the nucleophile attacks one of the terminal carbons of a cationic (π-allyl)metal complex.

Let us look first at the reaction between $Cp_2Mo(\eta^3\text{-allyl})^+$, **1**, and the anionic nucleophile $^-CH(COOH)_2$, **2**, a simplified model of malonate ion. The calculations suggest that the reaction between **1** and **2** takes place via a loose complex, presented in Figure 1. The distances between the allyl carbons and the anionic center of **2** are very long, and therefore, no covalent bond is formed at this stage. Figure 2 illustrates the transition-state structures for the attack of **2** to the central carbon of the allyl moiety in **1** and the attack of **2** to one of the terminal carbons of the allyl moiety. The C−C bond being formed is still very long at the transition state, 2.740 Å for the central attack and 2.539 Å for the terminal attack. In the attack of **2** to the central carbon of the allyl moiety in **1**, the distance between the central carbon and the molybdenum center gets longer, while the distances between the terminal carbons and the metal center become shorter. Though the changes in bond lengths are still small, one sees that the $Cp_2Mo(\eta^3\text{-allyl})^+$ part begins to be converted to a metallacyclobutane upon the attack of the nucleophile. On the other hand, in the terminal attack, the distance between the allyl carbon under attack and the molybdenum center becomes longer, whereas those between two other allyl carbons and the molybdenum center tend to become shorter, relative to those in the initial reactant complex. The $Cp_2Mo(\eta^3\text{-allyl})^+$ part begins to change its structure toward a η^2-complex.

The anionic charge in **2** is delocalized over the two carboxyl groups. The reaction site in **2** has been shown to have a relatively small negative net charge of −0.18 in the reactant complex.[29] It has been reduced to −0.15 at the transition state for the terminal attack and to −0.16 at the transition state for the central attack. The positive charge on the molybdenum center has been reduced from +1.78 in the reactant complex state to +1.74 at the transition state for the terminal attack and to +1.76 at the transition state for the central attack. The charge transferred from the attacking nucleophile appears to be housed temporarily on the metal center. The change in the charge distribution is not large, however, reflecting that the separation between **1** and **2** is still large at the transition states. Changes in the structure and electron distributions in the cyclopentadienyl ligands have been found to be negligibly small.

The calculated activation energy and heat of formation are given in Figure 2 and Figure 3. The barrier height for the central attack has been calculated to be 1.6 kJ/mol at the B3LYP/BS3//B3LYP/BS1 level (16.3 kJ/mol at the B3LYP/BS1 level), which is lower than that for the terminal attack, 18.3 kJ/mol (40.6 kJ/mol).[30] The results of theoretical calculations appear to agree with the experimental observation that nucleophiles attack preferentially the central carbon of an allyl unit to give metallacyclobutanes in the complexes having the form of $Cp_2M(\eta^3\text{-allyl})^+$ (M = Mo and W).[9,13] At the transition state for the central attack, one of the oxygens in the attacking nucleophile is located in a position that is favorable for bonding with one of the hydrogens of a terminal methylene of the allyl and with two hydrogens in a cyclopentadienyl ligand. This seems to contribute to the lower barrier height for the central attack, compared with that for the terminal attack, to some extent.

(27) (a) Ditchfield, R.; Hehre, W. J.; Pople, J. A. *J. Chem, Phys.* **1971**, *54*, 724. (b) Hehre, W. J.; Ditchfield, R.; Pople, J. A. *J. Chem. Phys.* **1972**, *56*, 2257.

(28) Illustration of the interaction orbitals was made by using the MOs calculated with Huzinaga's 21 split valence basis set (MIDI) for the complexes with the B3LYP/BS1 optimized structure. See: Huzinaga, S.; Andzelm, J.; Klobukowski, M.; Radzio-Andzelm, E.; Sakai, Y.; Tatewaki, H. *Gaussian Basis Sets For Molecular Calculations*; Elsevier: Amsterdam, 1984.

(29) Mulliken, R. S. *J. Chem. Phys.* **1955**, *23*, 1833, 1841, 2338, 2343.

(30) Among the reactant complex, two transition structures, and product complexes in the system of $Cp_2Mo(\eta^3\text{-allyl})^+$ and the nucleophile, the differences of zero-point correction were within 4.2 kJ/mol, and the differences of thermal correction to enthalpy were also within 4.2 kJ/mol. Both of these values are presented in the Supporting Information.

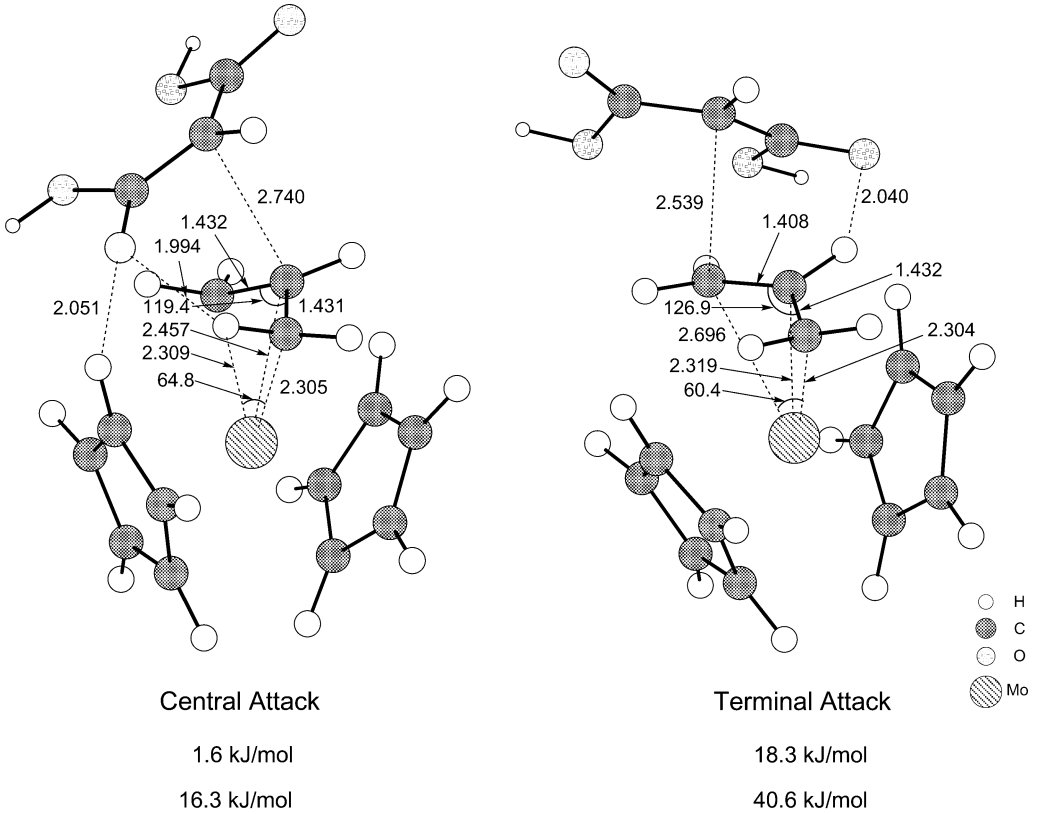

Figure 2. Transition-state structures for the attack of $^{-}CH(COOH)_2$ to the central carbon (left) and to one of the terminal carbons (right) of the allyl moiety of $Cp_2Mo(\eta^3\text{-allyl})^+$. Activation energy (kJ/mol) is given for the B3LYP/BS3//B3LYP/BS1 (above) and B3LYP/BS1 (below) calculations.

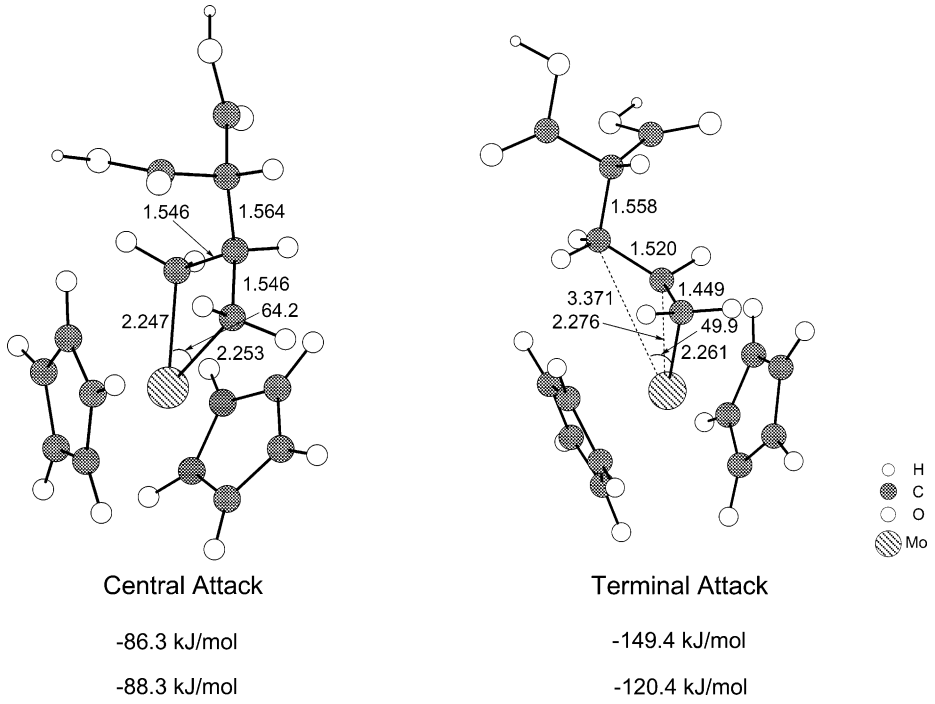

Figure 3. Structures of the products of the central and terminal attacks of $^{-}CH(COOH)_2$ to $Cp_2Mo(\eta^3\text{-allyl})^+$. Heat of formation (kJ/mol) is given for the B3LYP/BS3//B3LYP/BS1 (above) and B3LYP/BS1 (below) calculations.

The calculated structures of the products are presented in Figure 3. The product for the central attack has a metallacyclobutane form. The two C−C bonds have the typical single bond length, 1.546 Å, and the two C−Mo bonds are very similar in their lengths. The net charges on the carbons bound to the metal are −0.20 and −0.24, having been increased with the progress of the reaction from −0.08 and −0.12 in the reactant complex, respectively. The central carbon had a negative charge of −0.08 in the reactant state, but is almost neutral in the product.

The product of the terminal attack has the structure of a typical η^2-type complex. The two C−Mo bonds are very similar in their lengths, 2.261 and 2.276 Å. The

Scheme 3

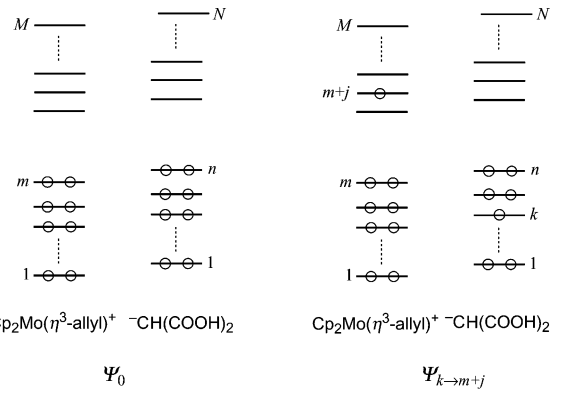

allylic C−C bonds have been elongated compared with those in the reactant complex or at the transition state. The net charge on the central carbon is −0.22, and that on the terminal carbon is −0.21. The reaction site of **1** has been shown to carry almost no net charge in the product. It is seen in Figure 3 that both reactions are exothermic and that the η^2-coordinated structure is more stable than the metallacyclic structure.

Orbital Interactions. To get a clearer view of interactions, let us look at the wave function for the reacting systems. We expand first the MO of a reacting system in a linear combination of the MOs of the two fragment systems, $Cp_2Mo(\eta^3\text{-allyl})^+$ and $^-CH(COOH)_2$, each frozen to the structure at the transition state. Then, the wave function of the reacting system is represented in a form of linear combination of various electron configurations of the two fragment species.[31] The coefficients that measure the contributions of those electron configurations to the electronic structure of the reacting system are determined by applying the method of configuration analysis.[32] The original electron configuration Ψ_0 in which both $Cp_2Mo(\eta^3\text{-allyl})^+$ and $^-CH(COOH)_2$ retain their electron configurations in an isolated state has been found to be the major term of the wave function. Orbital interactions are represented now in terms of the interactions between Ψ_0 and the configurations in which an electron is shifted from an occupied MO of the nucleophile to an unoccupied MO of the molybdenum complex, as illustrated in Scheme 3.[31] The nucleophile has many occupied MOs ψ_k ($k = 1, 2, ..., n$), and the metal complex has many unoccupied MOs, ϕ_{m+j} ($j = 1, 2, ..., M-m$).

We next carry out unitary transformations of the fragment MOs simultaneously within the unoccupied MO space of the $Cp_2Mo(\eta^3\text{-allyl})^+$ fragment and within the occupied MO space of the $^-CH(COOH)_2$ fragment, by utilizing the coefficients of electron-transferred configurations in the wave function. By this treatment, electron delocalization from the $^-CH(COOH)_2$ part to the $Cp_2Mo(\eta^3\text{-allyl})^+$ part expressed in terms of many electron-transferred configurations $\Psi_{k\rightarrow m+j}$ ($k = 1, 2, ..., n; j = 1, 2, ..., M-m$) in the canonical MO representation is summed up into a few terms in which delocalization of electrons takes place within the paired interaction orbitals of the two fragments (Scheme 3).[18] Not only the frontier MOs but also all the occupied MOs of the attacking nucleophile and all the unoccupied MOs of the complex are taken properly into account by this treatment.

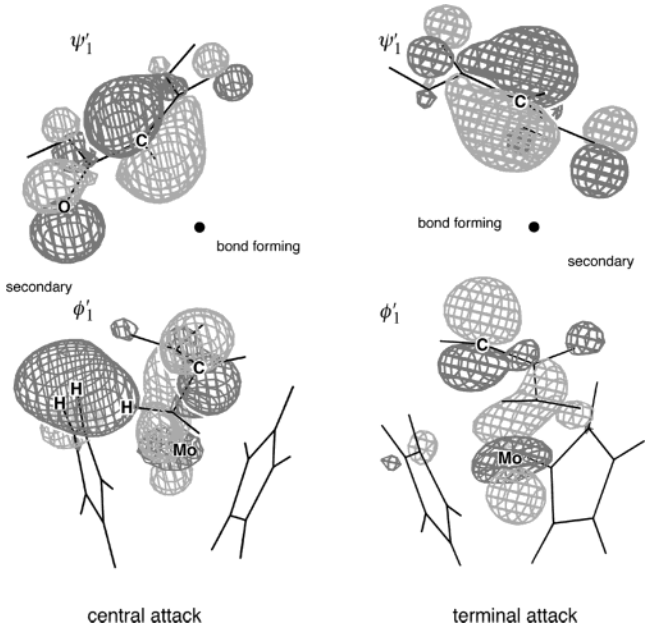

Figure 4. Orbital pair that participates in electron delocalization from the $^-CH(COOH)_2$ fragment to the $Cp_2Mo(\eta^3\text{-allyl})^+$ fragment at the transition state of the central attack (left) and at the transition state of the terminal attack (right). The orbital ψ'_1 of the attacking nucleophile is occupied and its counterpart orbital ϕ'_1 of the metal complex is unoccupied in each case. The relative location of $Cp_2Mo(\eta^3\text{-allyl})^+$ and $^-CH(COOH)_2$ at the transition state is obtained by moving the central carbon of the allyl moiety to the point marked by a dot.

In the present case, a pair of interaction orbitals has been demonstrated to play a dominant role at the transition state. The orbital pair derived for the central attack and that for the terminal attack are illustrated in Figure 4. The orbital ψ'_1 is given by a linear combination of the occupied canonical MOs of the $^-CH(COOH)_2$ fragment and the orbital ϕ'_1 is given by a combination of the unoccupied MOs of the $Cp_2Mo(\eta^3\text{-allyl})^+$ fragment in each case. Now, delocalization of electrons is represented by the mixing of Ψ_0 with an electron configuration that is generated by shifting an electron from ψ'_1 of the nucleophile to ϕ'_1 of the metal complex. In the central attack, the orbital ψ'_1 is seen to have a large amplitude on the anionic center of $^-CH(COOH)_2$. The paired orbital ϕ'_1 of the $Cp_2Mo(\eta^3\text{-allyl})^+$ part shows a large amplitude on the pπ AO of the central carbon under attack, but is delocalized to some extent over the p- and d-type AOs of the metal. An interesting feature of this orbital pair is that ϕ'_1 of $Cp_2Mo(\eta^3\text{-allyl})^+$ shows a significant amplitude on a terminal hydrogen of the allyl and two hydrogens in a cyclopentadienyl ligand. Thus, in addition to the *in-phase* overlap at the reaction sites, ϕ'_1 overlaps *in-phase* with ψ'_1 between these hydrogens and one of the oxygens in $^-CH(COOH)_2$. This should be one of the reasons why the activation energy calculated for the central attack is considerably lower than that for the terminal attack.

When the $^-CH(COOH)_2$ anion attacks one of the terminal carbons of $Cp_2Mo(\eta^3\text{-allyl})^+$, orbital interac-

(31) Fukui, K.; Fujimoto, H. *Bull. Chem. Soc. Jpn.* **1968**, *41*, 1989.
(32) Fujimoto, H.; Kato, S.; Yamabe, S.; Fukui, K. *J. Chem. Phys.* **1974**, *60*, 572.

tions are represented by the mixing in of the electron-transferred configuration in which an electron has been shifted from the anionic fragment to the metal fragment among the set of interaction orbitals, shown on the right-hand side of Figure 4. The orbital ψ'_1 of the attacking anion is seen to have almost the same shape as that obtained for the central attack. The unoccupied reactive orbital ϕ'_1 of the $Cp_2Mo(\eta^3\text{-allyl})^+$ fragment looks very different from that for the central attack, showing a large amplitude on the pπ AO of the terminal carbon under attack. The orbital is seen to have a small amplitude on the pπ AO of the central carbon and on the d-type AOs of the metal. As with the central attack, in addition to the *in-phase* orbital overlap at the reaction sites, ϕ'_1 overlaps *in-phase* with ψ'_1 between a terminal hydrogen of the allyl and one of the oxygens in $^-CH(COOH)_2$. The secondary *in-phase* orbital overlap will assist the reaction.

Reactive Orbitals and Reactivity of Active Sites. It has been shown above that the orbital of $Cp_2Mo(\eta^3\text{-allyl})^+$ that participates actually in electron delocalization from the attacking nucleophile is localized effectively on the pπ-type AO of the allyl carbon under attack, except that the central attack is accompanied by a secondary orbital interaction between an oxygen of the anion and several hydrogens in the complex. Those orbitals look significantly different from the 2a″ and 3a′ MOs mentioned above. This indicates that at least several canonical MOs of the complex participate in the interaction with the attacking nucleophile. To understand the difference in reactivity of the central and terminal carbons, we tried to generate the reactive orbitals for an isolated $Cp_2Mo(\eta^3\text{-allyl})^+$ system that retain the basic feature of the interaction orbitals obtained above.

It has been revealed that the pπ AO of the central carbon of allyl plays a key role in electron delocalization from the nucleophile in the central attack. We assume, therefore, that the p AO function of the central carbon extending in the direction equiangular from the two terminal carbons and the hydrogen attached to the central carbon atom in an isolated state of the complex gets primarily into the bond formation with the nucleophile (Scheme 4). We denote this orbital function by δ_r,

Scheme 4

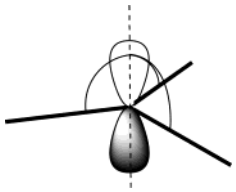

where r is the central carbon of the allyl moiety in the metal complex. For the terminal attack, we take a p AO of the carbon extending in the direction equiangular from the three bonds that connect the terminal carbon with the central carbon and with the two attached hydrogens in an isolated state of the complex as the reference orbital, δ_r. In this case, r indicates one of the terminal carbons. The combination of the inner and outer parts of the p AO in the double-ζ basis set has been taken as the same as that in the interaction orbital obtained above.[33]

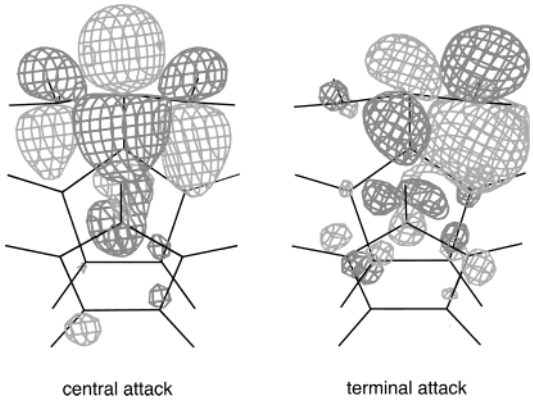

Figure 5. Projected unoccupied reactive orbitals for the central attack (left) and for the terminal attack (right).

The occupied and unoccupied MOs of a (π-allyl) complex in an isolated state are denoted again by ϕ_i ($i = 1, ..., m$) and ϕ_{m+j} ($j = 1, ..., M-m$), respectively. Then, by projecting δ_r onto the unoccupied MO space, we obtain the unoccupied reactive orbital ϕ_{unoc} that has the maximum amplitude on the referenced p AO.[19] The p AO has some populations also in the occupied MO space, and accordingly, the projection of δ_r onto the occupied MOs gives rise to the occupied reactive orbital ϕ_{oc} that has the maximum amplitude on δ_r,

$$\phi_{\mathrm{unoc}}(\delta_r) = \Big(\sum_{j=1}^{M-m} d_{m+j,r}\phi_{m+j}\Big)\Big/\Big(\sum_{j=1}^{M-m} d_{m+j,r}^2\Big)^{1/2} \qquad (1)$$

$$\phi_{\mathrm{oc}}(\delta_r) = \Big(\sum_{i=1}^{m} d_{i,r}\phi_i\Big)\Big/\Big(\sum_{i=1}^{m} d_{i,r}^2\Big)^{1/2} \qquad (2)$$

where the coefficients $d_{m+j,r}$ and $d_{i,r}$ are determined by expanding δ_r in terms of the occupied and unoccupied canonical MOs.

$$\delta_r = \sum_{i=1}^{m} d_{i,r}\phi_i + \sum_{j=1}^{M-m} d_{m+j,r}\phi_{m+j} \qquad (3)$$

The reactive orbitals projected out of the unoccupied MOs for the central and terminal attacks of nucleophiles are illustrated in Figure 5 for $Cp_2Mo(\eta^3\text{-allyl})^+$ in an isolated state. The reactive orbital shows the largest amplitude either on the central carbon or on a terminal carbon, depending on the p AO used as δ_r. It is seen, however, that the orbital is delocalized to some extent over the other carbons in both cases. The orbital for the central attack looks like the π_3 MO of an allyl or the 3a′ MO of the metal complex. In contrast, the reactive orbital for the terminal attack does not look like the π_2 MO of an allyl, but bears a resemblance to the π^* MO of an ethylene.[34] These orbitals will be transformed in

(33) The ratio of the inner and outer parts of the p AO function was approximately 1:4 in weight.

(34) The LUMO of $Cp_2Mo(\eta^3\text{-allyl})^+$ is symmetric and has an amplitude on the central carbon. However, this orbital has amplitudes on the metal center to some extent, and some higher unoccupied MOs have amplitudes on the central carbon. On the other hand, the LUMO of the complexes **3**, **4**, **6**, **7**, which prefer the terminal attack, have amplitudes on the terminal carbon. The features of the LUMOs are consistent with the attack position.

Table 1. Electron-Accepting Ability, Acidic Hardness, and Electronegativity of the Carbons in CpMo(π-Allyl)(CO)(NO)$^+$ and Other Molybdenum Complexes

species	λ	$2a^2\eta$	λ_{unoc}
$Cp_2Mo(\eta^3\text{-allyl})^+$			
C_c	−0.4459	0.5064	0.0605
C_t	−0.4381	0.5175	0.0794
$CpMo(\eta^3\text{-allyl})(CO)(NO)^+$ *exo*			
C_c	−0.5094	0.5519	0.0424
C_{t1} (*trans*)	−0.4681	0.4772	0.0091
C_{t2} (*cis*)	−0.4504	0.4330	0.0174
$CpMo(\eta^3\text{-allyl})(CO)(NO)^+$ *endo*			
C_c	−0.4877	0.5211	0.0334
C_{t1} (*trans*)	−0.4620	0.4609	−0.0011
C_{t2} (*cis*)	−0.4721	0.4693	−0.0028
$Mo(\eta^3\text{-allyl})(CO)_2(PH_3)_3^+$			
C_c	−0.4928	0.5915	0.0986
C_t	−0.4373	0.4884	0.0512
$Mo(\eta^3\text{-allyl})(CO)_2(PH_3)_2^+$			
C_c	−0.4923	0.5728	0.0805
C_{t1}	−0.4317	0.4621	0.0304
C_{t2}	−0.4633	0.5149	0.0517
$CpMo(C_4H_6)(CO)_2^+$ *endo* **8**			
C_b	−0.4813	0.5189	0.0376
C_t	−0.4575	0.4728	0.0153
$CpMo(C_4H_6)(CO)_2^+$ *exo* **9**			
C_b	−0.4955	0.5323	0.0368
C_t	−0.4533	0.4689	0.0155

the interaction with $^-CH(COOH)_2$, to give the interaction orbital ϕ'_1 at the transition state.

The reactive orbital ϕ_{unoc} obtained in this manner is given by a linear combination of the unoccupied canonical MOs of the complex, and therefore, the electron-accepting level λ_{unoc} of the reaction site r is estimated by taking the weighted sum of the orbital energies ϵ_{m+j} of the component unoccupied MOs in ψ_{unoc}.[19]

$$\lambda_{unoc}(\delta_r) = \left(\sum_{j=1}^{M-m} d^2_{m+j,r}\,\epsilon_{m+j}\right)/\left(\sum_{j=1}^{M-m} d^2_{m+j,r}\right) \qquad (4)$$

Similarly, the electron-donating ability λ_{oc} of the reaction site r is estimated by taking the sum of the orbital energies ϵ_i of the component occupied MOs.[19]

$$\lambda_{oc}(\delta_r) = \left(\sum_{i=1}^{m} d^2_{i,r}\,\epsilon_i\right)/\left(\sum_{i=1}^{m} d^2_{i,r}\right) \qquad (5)$$

Table 1 presents the λ_{unoc} values of the allyl carbons in $Cp_2Mo(\eta^3\text{-allyl})^+$. The central carbon has the unoccupied reactive orbital located considerably lower in energy, compared with that for the terminal carbons. This indicates clearly that the central carbon has a stronger ability for electron acceptance in an isolated state of $Cp_2Mo(\eta^3\text{-allyl})^+$. Central attack of nucleophiles is more favored in $Cp_2Mo(\eta^3\text{-allyl})^+$, in agreement with experiments,[9,13] with or without assistance of the secondary orbital interactions depicted above.

The electron-accepting level λ_{unoc} is controlled by two terms, λ and $2a^2\eta$, as sketched in Scheme 5.[19b] The former is given by $\lambda = a^2\lambda_{oc} + (1 - a^2)\lambda_{unoc}$ in which $(1 - a^2)$ and a^2 are equal to the denominator of eq 4 and eq 5, respectively. The projected reactive orbital has been determined so as to have the maximum amplitude on the reference orbital δ_r, but the orbital is delocalized more or less over the neighboring atoms. The portion of ϕ_{unoc} that cannot be utilized for the bond formation at the reaction site with the attacking nucleophile is a^2

Scheme 5

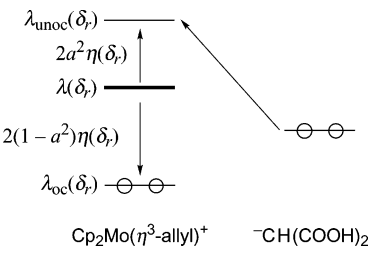

($a^2 \leq 1$). A larger a^2 value indicates that the bond formation with a nucleophile is weaker at that site. One-half of the gap between the electron-accepting level λ_{unoc} and the electron-donating level λ_{oc} of the reaction site r is denoted here by η, i.e., $\eta = (\lambda_{unoc} - \lambda_{oc})/2$. This is analogous in a mathematical sense to the chemical hardness defined for a molecule by Parr, $(I - A)/2 \cong (\epsilon_{LUMO} - \epsilon_{HOMO})/2$ where I and A represent the ionization potential and the electron affinity of a molecule, respectively, and ϵ_{LUMO} and ϵ_{HOMO} signify the orbital energy of the LUMO and of the HOMO, respectively.[35] A larger η value indicates that the reaction site r is less polarizable. The term $2a^2\eta$ is regarded then as specifying hardness of the reaction site r against electron acceptance and, accordingly, as specifying hardness of the reaction site as a Lewis acid in a reactant molecule. It measures how far the electron-accepting level λ_{unoc} is located above λ.

The electronegativity of a molecule was defined by Mulliken in terms of $(I + A)/2 \cong -(\epsilon_{HOMO} + \epsilon_{LUMO})/2$.[36] If we place $a^2 = 1/2$ in Scheme 5 for a reaction site r which serves both as an electron acceptor and as an electron donor to a similar extent, we obtain $-\lambda = -(\lambda_{oc} + \lambda_{unoc})/2$. From the formal similarity, $-\lambda$ is regarded as representing the electronegativity of the carbon r in an allyl cation coordinated to the metal complex.[37] In the case of the reaction site r, a^2 can change between 0 and 1 to specify whether the reaction site behaves more like an acid or more like a base. The location of λ is sensitive to the electronic charge on the reaction site, while the acidic hardness term $2a^2\eta$ depends primarily on the orbitals that are utilized for the formation of new bonds. Table 1 shows that λ is located slightly lower and the hardness term is smaller at the central carbon in the $Cp_2Mo(\eta^3\text{-allyl})^+$ complex. As a result, the central carbon has a lower λ_{unoc} value compared with the terminal carbons, indicating that the central carbon is softer as a Lewis acid in this complex primarily due to its stronger polarizability.

$CpMo(\eta^3\text{-allyl})(CO)(NO)^+$ and Other Molybdenum Complexes. Let us next look at another molybdenum complex, $CpMo(\eta^3\text{-allyl})(CO)(NO)^+$. The structures and relative energies of three $CpMo(\eta^3\text{-allyl})(CO)(NO)^+$ isomers calculated at the B3LYP/BS1 level are given in Figure 6. The *exo* isomer **4** is seen to be slightly more stable than the *endo* isomer **3**. Conformational equilibrium between the two isomers was suggested more than 20 years ago,[11,38,39] but the mechanism has not yet been clarified well. A $\sigma-\pi-\sigma$ conversion and an allyl rotation have so far been proposed.[11]

(35) Parr, R. G.; Zhou, Z. *Acc. Chem. Res.* **1993**, *26*, 256.
(36) Mulliken, R. S. *J. Chem. Phys.* **1934**, *2*, 782.
(37) Pauling, L. *The Nature of the Chemical Bond*; Cornell University Press: Ithaca, NY, 1960.

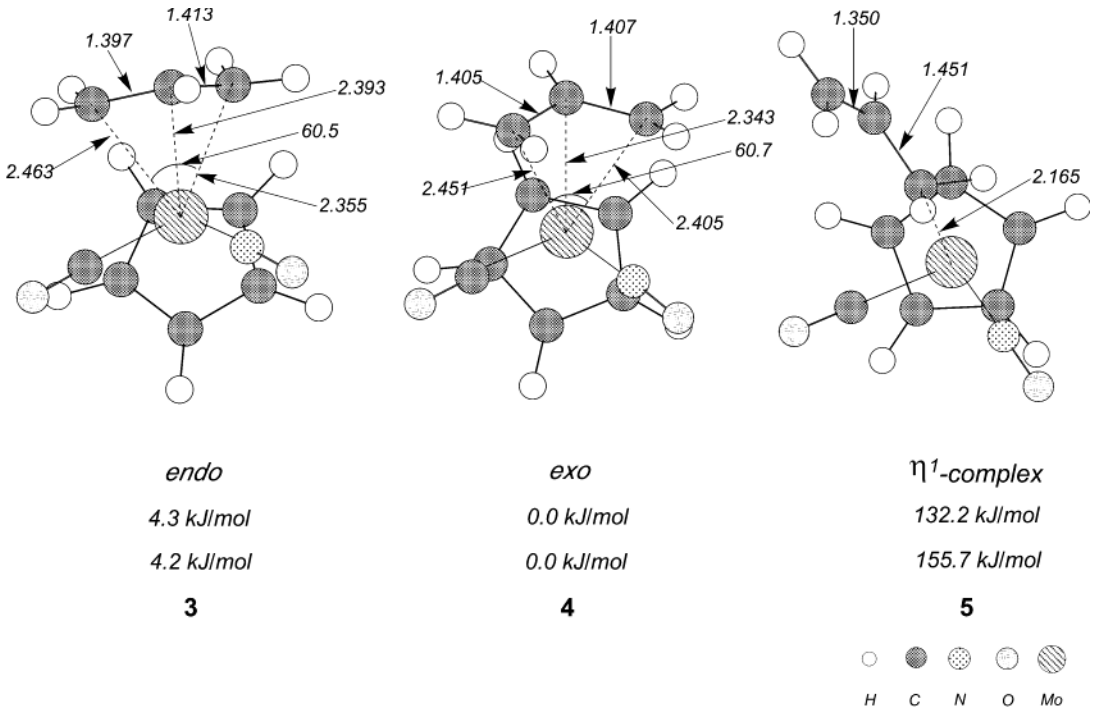

Figure 6. Calculated structures of the *endo*, *exo*, and η^1-isomers of the CpMo(η^3-allyl)(NO)(CO)$^+$ complex. Relative energies (kJ/mol) are given for the B3LYP/BS3//B3LYP/BS1 (above) and B3LYP/BS1 (below) calculations.

The present calculations show that the η^1-complex structure **5** is very unstable relative to the η^3-complexes. This makes a big difference from (allyl)Pd(PH_3)$_2$ and (allyl)Pt(PH_3)$_2$, in which the η^1-complex has been located above the η^3-complexes by 43 kJ/mol in the former and only by 11 kJ/mol in the latter.[40] It is suggested, therefore, that interconversion between the η^3-complexes in CpMo(η^3-allyl)(CO)(NO)$^+$ should take place not through the η^1-complex but through an allyl rotation.

The terminal allylic carbon *trans* to the NO ligand is most reactive in the *endo* isomer, whereas the terminal carbon *cis* to the NO ligand is most reactive in the *exo* isomer.[5c−h,6] We have calculated λ_{unoc} values for the allylic carbons in CpMo(η^3-allyl)(CO)(NO)$^+$, as presented in Table 1. In contrast to the case of $Cp_2Mo(\eta^3\text{-allyl})^+$, the terminal carbons have lower λ_{unoc} values than the central carbon and, therefore, should be more reactive toward nucleophiles. The terminal carbon *cis* to the NO ligand is seen to have an unoccupied reactive orbital which is considerably lower in energy than that of the carbon *trans* to the NO ligand in the *exo* isomer, indicating that the terminal carbon *cis* to the NO ligand is more reactive. On the other hand, two terminal carbons are suggested to be comparable in the electron-accepting ability in the *endo* isomer. This does not agree with the experimental observation. To see the difference, we have calculated the activation energy for the addition of $^-CH(COOH)_2$ to the *endo* isomer of CpMo(η^3-allyl)(CO)(NO)$^+$. The transition-state structures are illustrated in Figure 7. The attack to the carbon *cis* to the NO ligand has been shown to have an activation energy higher than the addition to the carbon *trans* to the NO ligand, but only by 4.2 kJ/mol. Though it seems to be difficult to interpret all of the experimental observations consistently within the present reaction models, it is interesting to see that the Lewis acidity of the central and terminal carbons is reversed by the ligands attached to the metal center.

We refer next to hexacoordinated complexes, MoX(η^3-allyl)(CO)$_2$L$_2$. Their structures and characters have been investigated since some 30 years ago.[41−43] In particular, the regio- and chemoselectivities in the reactions of these complexes have been studied by Trost et al.,[7,8] as illustrated below. Some differences in regioselectivity are seen to be brought about by the position of the halogen ligand (Scheme 6).[44]

The starting materials and the products have been well identified, but the reactant species for the nucleophilic attack have not been clarified well.[8] The reactions were carried out in an excess of phosphine. The halogen ligand in the complex may be replaced by a phosphine. In the hexacoordinated Mo(η^3-allyl)(CO)$_2$(PH_3)$_3^+$, **6**, in

(38) (a) Faller, J. W.; Incorvia, M. J. *Inorg. Chem.* **1968**, *7*, 840. (b) Faller, J. W.; Jakubowski, A. *J. Organomet. Chem.* **1971**, *31*, C75. (c) Faller, J. W.; Chen, C. C.; Mattina, M. J.; Jakubowski, A. *J. Organomet. Chem.* **1973**, *52*, 361. (d) Faller, J. W.; Chodosh, D. F.; Katahira, D. *J. Organomet. Chem.* **1980**, *187*, 227.

(39) (a) Davison, A.; Rode, W. C. *Inorg. Chem.* **1967**, *6*, 2124. (b) Vinson, N. A.; Day, C. S.; Welker, M. E.; Guzei, I.; Rheingold, A. L. *Organometallics* **1999**, *18*, 1824.

(40) Suzuki, T.; Fujimoto, H. *Inorg. Chem.* **1999**, *38*, 370.

(41) (a) Hull, C. G.; Stiddard, M. H. B. *J. Organomet. Chem.* **1967**, *9*, 519. (b) Hayter, R. G. *J. Organomet. Chem.* **1968**, *13*, P1. (c) Dieck, H. T.; Friedel, H. *J. Organomet. Chem.* **1968**, *14*, 375. (d) Holloway, C. E.; Kelly, J. D.; Stiddard, M. H. B. *J. Chem. Soc., A* **1969**, 931. (e) Faller, J. W.; Haitko, D. A.; Adams, R. D.; Chodosh, D. F. *J. Am. Chem. Soc.* **1979**, *101*, 865.

(42) (a) Brisdon, B. J.; Griffin, G. F. *J. Chem. Soc., Dalton Trans.* **1975**, 1999. (b) Brisdon, B. *J. Organomet. Chem.* **1977**, *125*, 225. (c) Brisdon, B. J.; Edwards, D. A.; White, J. W. *J. Organomet. Chem.* **1978**, *156*, 427. (d) Drew, M. G. B.; Brisdon, B. J.; Edwards, D. A.; Paddick, K. E. *Inorg Chim Acta* **1979**, *35*, L381.

(43) Brisdon, B. J.; Griffin, G. F. *J. Organomet. Chem.* **1974**, *76*, C47.

(44) Trost et al. proposed that cationic species should be more susceptible to nucleophilic attack in ref 8. So we investigated cationic species that are formed by eliminating a halogen ligand. In these species, the relative reactivities of two terminal carbons of the allyl group should affect the vacant site which is located *cis* to the allyl group.

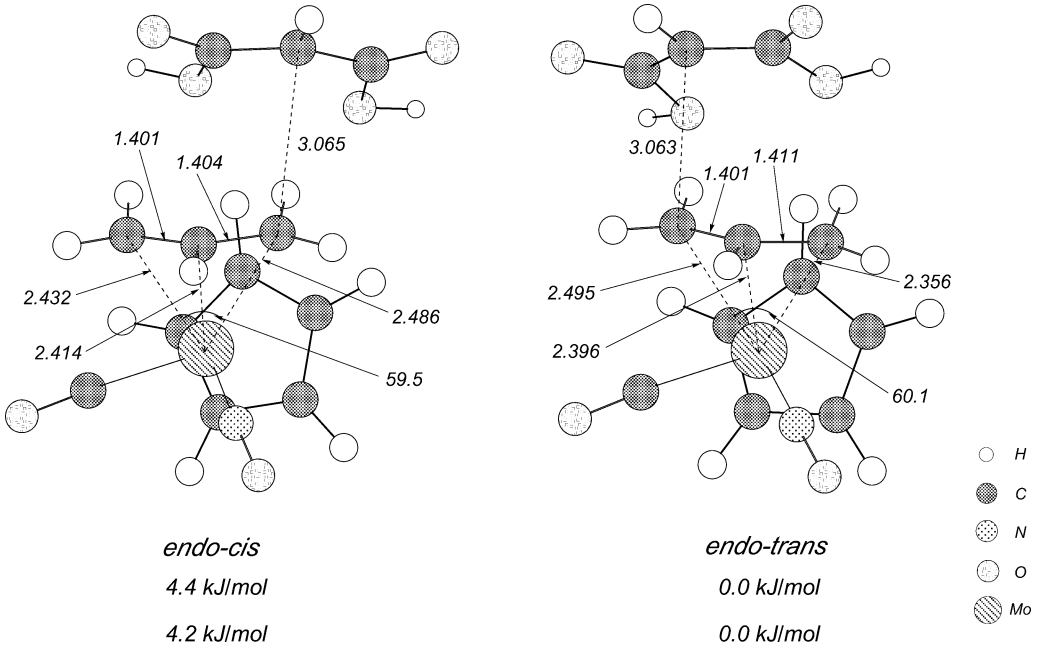

Figure 7. Transition-state structures for the addition of $^{-}CH(COOH)_2$ to the terminal carbons of the *endo* isomer of the $CpMo(\eta^3\text{-allyl})(NO)(CO)^+$ complex. Relative energies (kJ/mol) are given for the B3LYP/BS3//B3LYP/BS2 (above) and B3LYP/BS2 (below) calculations.

Scheme 6

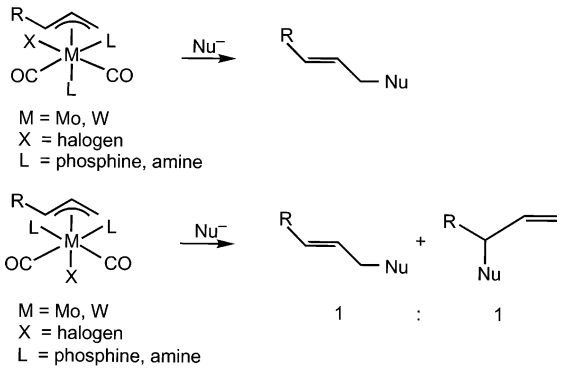

which the phosphine ligands in real systems have been modeled by PH_3, the terminal carbons are shown in Table 1 to have a considerably lower λ_{unoc} value compared with that of the central carbon. Also in $Mo(\eta^3\text{-allyl})(CO)_2(PH_3)_2^+$, **7**, in which the halogen ligand has been eliminated, the terminal carbons have considerably lower λ_{unoc} values. These results are in line with the observed reactivity trend that nucleophiles attack preferentially the terminal carbons.[8] Among the two terminal carbons C_{t1} and C_{t2} in **7**, the former, which is located farther apart from the vacant site, is shown to be more reactive. When the allyl moiety carries a substituent, the substituent will be attached to the terminal carbon C_{t2}, which occupies the less-hindered site. The alkyl substituents do not affect significantly the electron-accepting ability of the carbons.[45] Thus, assuming **7** to be an active species in this reaction, the addition of nucleophiles to the terminal carbon without the substituent is suggested to be the major process, in accordance with the experiments.[7,8]

Finally, we discuss $CpMo(diene)(CO)_2^+$ complexes. These complexes are known to be attacked by nucleophiles to yield the reactant species $CpMo(\eta^3\text{-allyl})(CO)(NO)^+$. The regio- and stereoselectivities to give cyclic diene complexes have been reported.[46,47]

The *endo* isomer **8** has been calculated to be more stable than the *exo* isomer **9** by 8.2 kJ/mol at the B3LYP/BS2//B3LYP/BS1 level. In both cases, the terminal carbons C_t of the diene unit have considerably lower

Chart 1

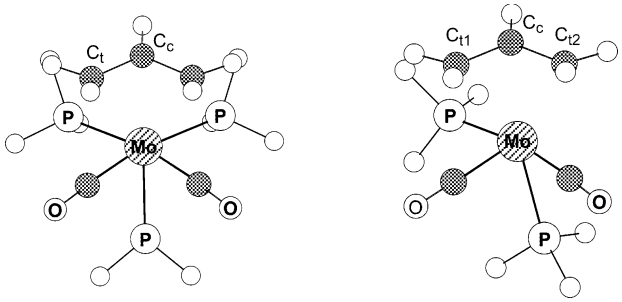

$Mo(\eta^3\text{-allyl})(CO)_2(PH_3)_3^+$ **6**

$Mo(\eta^3\text{-allyl})(CO)_2(PH_3)_2^+$ **7**

Scheme 7

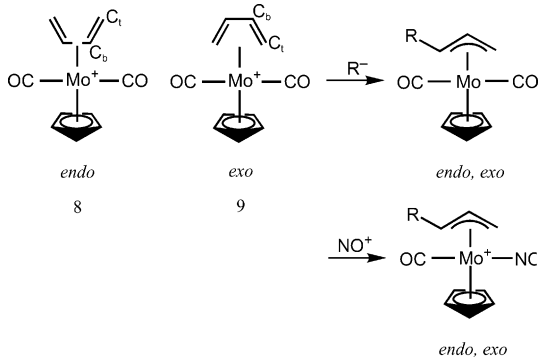

(45) Methyl substitution at a terminal carbon of the allyl unit in $Cp(\eta^3\text{-allyl})(CO)(NO)^+$ has shown that the carbons are made slightly less reactive, but the trend in reactivity remains the same.

λ_{unoc} values compared with that of the backbone carbons C_b. The reactivities of carbons in butadiene have not been changed by the coordination to the metal in this case. This should be one of the reasons why the terminal attack of nucleophiles is more favored.[46−51]

Conclusion

Reactivities of allyl carbons in (π-allyl)molybdenum complexes toward nucleophilies have been investigated theoretically. Orbital interactions have been elucidated by examining the wave functions of the theoretically determined transition-state structures of a reaction model, which consists of $Cp_2Mo(\eta^3\text{-allyl})^+$ and $^-CH(COOH)_2$. Unoccupied reactive orbitals that have the largest amplitude on the pπ AO of the central allylic carbon or on one of the terminal allylic carbons have then been derived for the $Cp_2Mo(\eta^3\text{-allyl})^+$ complex in an isolated state as the origin of the interaction orbitals. By utilizing these reactive orbitals projected out of the unoccupied MO space for the central and terminal carbons, the electron-accepting ability has been shown to be stronger at the central carbon in $Cp_2Mo(\eta^3\text{-allyl})^+$. This indicates that the formation of metallacyclobutane is favored, in agreement with the result of density functional theoretical calculations and with the experimental observations. In $CpMo(\eta^3\text{-allyl})(CO)(NO)^+$, on the other hand, the terminal carbons show higher abilities for electron acceptance. In the *exo* form, the terminal carbon that is *cis* to the NO ligand has a higher ability for electron acceptance, in agreement with the experiments. On the other hand, the two terminal carbons show similar nucleophilicity in the *endo* form.

The electron-accepting ability has been demonstrated to be controlled by two terms, electronegativity and acidic hardness of the reaction site. In the systems examined in the present study, the reactivity of allyl carbons has been shown to be determined mainly by the acidic hardness of each site. This signifies that the regioselectivity of the reactions is governed primarily by orbital interactions. The visualization of interactions between the reagent and the reactant by means of paired interaction orbitals and prediction of the reactivity of local sites in metal complexes in terms of electron-accepting or -donating ability will be of use in designing new templates for highly selective organic syntheses.

Acknowledgment. This work was supported in part by a Grant-in-Aid for Scientific Research by the Ministry of Education, Science, Sports and Culture of Japan. A part of the calculations was carried out at the Institute for Molecular Science under generous permission to use the Computer Center.

Supporting Information Available: Tables listing atomic positional parameters. This material is available free of charge via the Internet at http://pubs.acs.org.

OM0207459

(46) (a) Pearson, A. J.; Khan, M. N. I.; Clardy, J. C.; Chu-heng, H. *J. Am. Chem. Soc.* **1985**, *107*, 2748. (b) Pearson, A. J.; Khan, M. N. I. *J. Org. Chem.* **1985**, *50*, 5276. (c) Pearson, A. J.; Blystone, S. L.; Nar, H.; Pinkerton, A. A.; Roden, B. A.; Yoon, J. *J. Am. Chem. Soc.* **1989**, *111*, 134. (d) Pearson, A. J.; Kbetani, V. D. *J. Am. Chem. Soc.* **1989**, *111*, 6778. (e) Pearson, A. J.; Mallik, S.; Pinkerton, A. A.; Adams, J. P.; Zheng, S. *J. Org. Chem.* **1992**, *57*, 2910.

(47) Faller, J. W.; Murray, H. H.; White, D. L.; Chao, K. H. *Organometallics* **1983**, *2*, 400.

(48) Hansson, S.; Miller, J. F.; Liebeskind, L. S. *J. Am. Chem. Soc.* **1990**, *112*, 9660.

(49) Liebeskind, L. S.; Bombrun, A. *J. Am. Chem. Soc.* **1991**, *113*, 8736.

(50) Rubio, A.; Liebeskind, L. S. *J. Am. Chem. Soc.* **1993**, *115*, 891.

(51) Gamelas, C. A.; Herdtweck, E.; Lopes, J. P.; Romão, C. C. *Organometallics* **1999**, *18*, 506.